PRMS: Phase and RSSI based Localization System for Tagged Objects on Multilayer with a Single Antenna

Huatao Xu
School of Software, Shanghai Jiao Tong University, China
xuhuatao@sjtu.edu.cn

Run Zhao
Department of Computer Science and Engineering, Shanghai Jiao Tong University, China
zhaorun@cs.sjtu.edu.cn

Qian Zhang
School of Software, Shanghai Jiao Tong University, China
qwert3472@sjtu.edu.cn

Dong Wang*
School of Software, Shanghai Jiao Tong University, China
wangdong@sjtu.edu.cn

ABSTRACT

In the future, libraries and warehouses will gain benefits from the spatial location of books and merchandises attached with RFID tags. Existing localization algorithms, however, usually focus on improving positioning accuracy or the ordering one for RFID tags on the same layer. Nevertheless, books or merchandises are placed on the multilayer in reality and the layer of RFID tagged object is also an important position indication. To this end, we design PRMS, an RFID based localization system which utilizes both phase and RSSI values of the backscattered signal provided by a single antenna to estimate the spatial position for RFID tags. Our basic idea is to gain initial estimated locations of RFID tags through a basic model which extracts the phase differences between received signals to locate tags. Then an advanced model is proposed to improve the positioning accuracy combined with RF hologram based on basic model. We further change traditional deployment of a single antenna to distinguish the features of RFID tags on multilayer and adopt a machine learning algorithm to get the layer information of tagged objects. The experiment results show that the average accuracy of layer detection and sorting at low tag spacing (2 ∼ 8cm) are about 93% and 84% respectively.

CCS CONCEPTS

• **Information systems** → *Location based services*;

KEYWORDS

RFID, Localization, SAR, SVM

ACM Reference Format:
Huatao Xu, Run Zhao, Qian Zhang, and Dong Wang. 2018. PRMS: Phase and RSSI based Localization System for Tagged Objects on Multilayer with a Single Antenna. In *21st ACM International Conference on Modelling, Analysis and Simulation of Wireless and Mobile Systems (MSWIM '18), October 28-November 2, 2018, Montreal, QC, Canada.* ACM, New York, NY, USA, 5 pages. https://doi.org/10.1145/3242102.3242138

*Dong Wang is the corresponding author.

MSWIM '18, October 28-November 2, 2018, Montreal, QC, Canada

ACM ISBN 978-1-4503-5960-3/18/10…$15.00
https://doi.org/10.1145/3242102.3242138

1 INTRODUCTION

Nowadays, with the progress of integration between manufacturing technology and information technology, Radio Frequency Identification (RFID) has got broad applications owing to its merits of low cost and easy deployment which deeply influences the way of production and storage of goods in factories and warehouses. Early RFID based localization systems[4, 5] utilized received signal strength (RSS) to locate RFID tags and many schemes are proposed to improve the overall positioning or sorting accuracy. In recent years, many works use phase which reflects the propagation distance of signal to make localization for tags. Angle of arrival(AOA) based positioning techniques[1, 7] analysed the phase difference between the received signals for localization. Synthetic aperture radar (SAR) methods which are firstly used in Radar system are also applied to RFID localization[9, 13, 14]. Later researchers generated holography imaging which provides the spatial probability density function that reveals the actual RFID tag position to improve the positioning accuracy[8, 10, 15].

Nevertheless, prior works[10] mostly focus on the accuracy in one-dimension such as determining the order of tagged objects on the conveyor belt. Suppose some books attached with tags are placed on the different layers of a bookshelf, these algorithms can give the left-to-right order of each book among multilayer or the spatial location of it. However, the layer of book is still hard to decide, which is also an important item of positional information. HMRL[12] distinguishes the layer for tagged objects but it requires multi-antenna. Former work[11] makes it using a single antenna based on an assumption that the radial distances (the distance from tag to the trajectory of antenna in Figure 1) from different layers to antenna vary as shown in Figure 1 (e.g. $y_3 < y_4 < y_2 < y_1$). However, this hypothesis may be hard to establish when antenna is placed between the multilayer. A little change for the height of antenna may make the distance of one layer close to another's and it is detrimental for the deployment of system. Another alternative is to place the antenna at position P_1 or P_3 to vary the radical distances but the farthest layer will suffer signal loss due to the high altitude of bookshelf which we will discuss in the evaluation.

In this paper, to investigate whether a single moving antenna can obtain both the layer and order of target tags on the shelf, we design

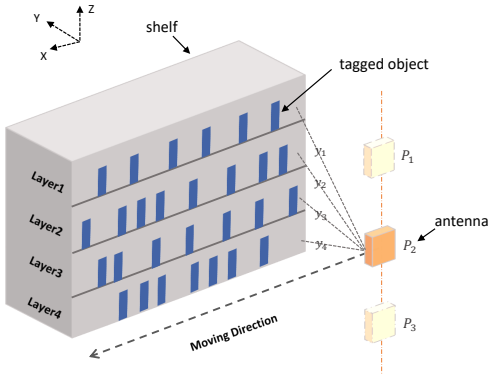

Figure 1: Traditional Localization Model via mobile scanning. (y_i stands for radial distance from tag on layer i to the antenna and P_1, P_3 are virtual locations with different height.)

PRMS, a synthetic aperture RFID localization system which takes advantage of both phase and RSSI profiles provided by the passive tags. In designing such a system, we faced several technical challenges. The first challenge is how to acquire the relative locations of RFID tags to the single reader antenna with high precision. For this, we propose a phase-based localization model which utilizes AoA profiles and optimize it by holography imaging to obtain more accurate estimated position.

Another key technical challenge is how to distinguish the tags on different layers with only one antenna. To combat this challenge, we change the traditional deployment of the unique antenna smartly and distinguish the multilayer utilizing both phase and RSSI values in the received signals even if there exist two layers owning similar or even same radial distance to the antenna. We could transfer the layer determination problem into a classification one because the number of layers is a determined small value (typically $3 \sim 5$) for a shelf. Besides, libraries or warehouses always purchase shelves with uniform specification and place them uniformly for unified management. This provides a possibility that we could solve the classification problem using a machine learning algorithm since the each layer shares the same height and similar surroundings among the different shelves.

2 PHASE-BASED LOCALIZATION MODELING

2.1 Basic Localization Model

Angle Profiles. As shown in Figure 2(a), an antenna which moves along the X-axis queries the target tag T at different positions A_i and A_{i+1} along a line separated by Δx_i ($\Delta x_i = x_{i+1} - x_i$). A_i and A_{i+1} form a point pair in our paper (e.g. A_2, A_3 is a point pair while A_2, A_4 isn't one) and each point pair contains two points while one point shows up in two point pairs at most. Let M_i be the middle point of A_i and A_{i+1} and α_i be the included angle between line TM and line A_iA_{i+1}, which is also the AoA of tag T. We use $d(T, A_i)$ to stand for the distance from tag T to A_i , and θ_i to represent the collected phase at A_i. Then the relation between $d(T, A_i)$ and θ_i can be written as follows:

$$\theta_i = (\frac{2\pi}{\lambda} \times 2d(T, A_i) + \varphi_i) \bmod 2\pi \tag{1}$$

Then the distance difference between $d(T, A_i)$ and $d(T, A_{i+1})$ can be defined as:

$$\Delta d_i = d(T, A_i) - d(T, A_{i+1}) = \frac{\lambda}{4\pi}(\theta_i - \theta_{i+1} + \delta_i + 2k_i\pi) \tag{2}$$

where $\delta_i = \varphi_i - \varphi_{i+1}$ and k_i is an integer. Since we use the same antenna to query the same target tag, φ_i is close to φ_{i+1}, which means δ_i is 0 or a small constant near 0. Then δ_i can be eliminated and Equation 2 could be simplified as:

$$\Delta d_i = \frac{\lambda}{4\pi}(\theta_i - \theta_{i+1} + 2k_i\pi) \tag{3}$$

If $|y_t| \gg |\Delta x_i|$, Δd_i can also be approximated as $\Delta d_i = \Delta x_i \times \cos\alpha_i, \alpha_i \in (0, \pi)$. Therefore $\cos\alpha_i$ can be expressed as:

$$\cos\alpha_i = \frac{\lambda}{2\Delta x_i} \times [\frac{\theta_i - \theta_{i+1}}{2\pi} + k_i] \tag{4}$$

Next, we consider about the value of k_i. It is obvious that $\cos\alpha_i \in (-1, 1)$, then k_i is within $(-\frac{\theta_i - \theta_{i+1}}{2\pi} - \frac{2\Delta x_i}{\lambda}, -\frac{\theta_i - \theta_{i+1}}{2\pi} + \frac{2\Delta x_i}{\lambda})$ and its range is $\frac{4\Delta x_i}{\lambda}$ according to the Equation 4. So we can control the value of k_i by reducing the value of Δx_i. If $\Delta x_i < \lambda/4$, which we call *Gap Constraint* at the rest of this paper, the range of k_i will be smaller than 1 , which means that k_i has a unique integer value. Moreover, this constraint also eliminates phase ambiguity and make sure that the phase difference between two consecutive measurements can be confined within 2π according to Triangle Constraint[7].

Linear Fitting. Then we convert $\cos\alpha_i$ to $\cot\alpha_i$. Considering the geometric relation in Figure 2(a), $\cot\alpha_i$ can be calculated by coordinate of target tag $T(x_t, y_t)$ and the middle point $M_i(\frac{x_i + x_{i+1}}{2}, 0)$:

$$\cot\alpha_i = \frac{x_t}{y_t} - \frac{\bar{x}_i}{y_t}, \bar{x}_i = \frac{x_i + x_{i+1}}{2} \tag{5}$$

As the antenna moves forward along the synthetic aperture, the $\bar{x}_i$ increases while $\cot\alpha_i$ decreases continuously, which is shown in Figure 2(a) intuitively. The $\cot\alpha_i$ of these orange points are extracted from phases and position data in adjacent point pairs. It is obvious that there is a typical linear relationship between $\bar{x}_i$ and $\cot\alpha_i$. In Equation 5, there are only two unknown parameters: x_t and y_t, which can be estimated by linear fitting with angle profiles and coordinates of corresponding middle points.

Preprocessing. The raw phase measurements are processed by unwrapping[6] firstly to remove the periodic change of phase values. After unwrapping, k_i will be a constant 0 theoretically if Δx_i satisfies the *Gap Constraint* all the time. Suppose we get two vector of phases and x-coordinates collected from measuring points:

$$\boldsymbol{s} = [\theta_1, \theta_2, ..., \theta_{n_r}]^T, \boldsymbol{x} = [x_1, x_2, ..., x_{n_r}]^T \tag{6}$$

where n_r is the number of measuring points. During experiments, some point pairs might obtain $|\Delta d|$ larger than $|\Delta x|$ even though their Δx satisfy *Gap Constraint*, which is caused by some dirty points existing in these point pairs. Since it is difficult to decide which point is dirty at one pair yet, we design a simple method to remove the improper pairs rather than concrete dirty points:

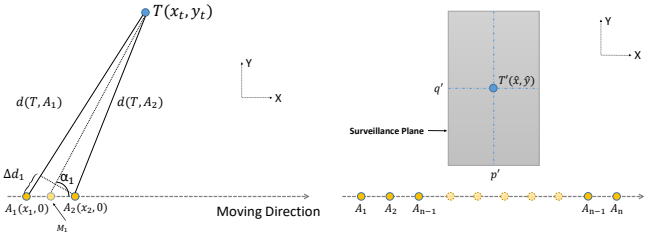

(a) AoA as the antenna moves (b) Surveillance Plane

Figure 2: Localization Model

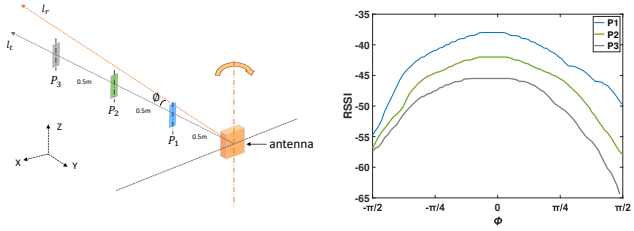

(a) Experiment Setting (b) AoA vs. RSSI

Figure 3: The relation between RSSI values and Angle of Arrival. (a) The antenna rotates along the Z-axis and the same tag is put at position P_1, P_2, P_3 respectively. ϕ represents the included angle between line l_r and l_t.

First, construct a $(n_r - 1) \times n_r$ null matrix $\boldsymbol{B}$. Second, assign some specific elements of $\boldsymbol{B}$ to record the pairs information using following *Pair Rule*: $\boldsymbol{B}_{i,i} = 1, \boldsymbol{B}_{i,i+1} = -1$ if $\frac{\lambda}{4\pi}(\boldsymbol{s}_i - \boldsymbol{s}_{i+1}) < \boldsymbol{x}_{i+1} - \boldsymbol{x}_i, i \in [1, n_r - 1]$. At last, process $\boldsymbol{B}$ by removing all the rows and columns without any non-zero value. Specially, if all elements in k^{th} column are equal to 0, then both two point pairs containing the k^{th} measuring point are improper, which means it is much likely to be a dirty point. And the k^{th} element in $\boldsymbol{s}$ and $\boldsymbol{x}$ will also be deleted simultaneously.

2.2 Advanced Localization Model

To evaluate the accuracy of basic localization model, we make several experiments and results shows the radial localization precision is not stable which can be proved through Equation 5 that y_t is easily influenced by little change of $\cot \alpha_i$. Therefore we design an advanced model to improve the performance based on the estimated position obtained from basic model.

Besides employing AoA information for localization, holography imaging is another effective method to locate tag and it achieves higher accuracy[15]. Suppose we get vector $\boldsymbol{s}$, $\boldsymbol{x}$ with length n and matrix $\boldsymbol{B}$ with dimension $m \times n$ after preprocessing, where m is the number of proper point pairs while n is the amount of clean measuring points. And we use $(\hat{x}, \hat{y})$ to represent the estimated localization obtained from basic model. The surveillance plane is partitioned into $P \times Q$ grids at cm level as illustrated in Figure 2(b). Orange points represent the observation points and T' stands for the estimated position obtained from basic model which is at the central grid of surveillance plane. Then the corresponding RF hologram $\boldsymbol{H}$ can be expressed as following image:

$$\boldsymbol{H} = \begin{bmatrix} h_{1,1} & \cdots & h_{1,q} \\ \vdots & \ddots & \vdots \\ h_{p,1} & \cdots & h_{p,q} \end{bmatrix}$$

where each pixel $h_{p,q} \in \boldsymbol{H}$ is used to indicate the likelihood of corresponding grid and mapped to a grid $Z_{p,q}$. The centroid of each grid is its coordinate. Then we define $\boldsymbol{t}_{p,q}$ to represent the theoretical phase differences for all point pairs if the signal is reflected at grid $Z_{p,q}$:

$$\boldsymbol{t}_{p,q} = \frac{4\pi}{\lambda} \times \boldsymbol{B}\, \boldsymbol{d}_{p,q} \tag{7}$$

where vector $\boldsymbol{d}_{p,q}$ with a length of n represents the distances from the centroid of grid $Z_{p,q}$ to each position A_i corresponding to the i^{th} element in $\boldsymbol{s}$ and $\boldsymbol{x}$. Next, let $\boldsymbol{a}$ be the actual phase differences for all point pairs:

$$\boldsymbol{a} = \boldsymbol{B}\, \boldsymbol{s} \tag{8}$$

Finally, the $h_{p,q}$ is defined as followed:

$$h_{p,q} = e^{-\sum_{i=0}^{m} (\boldsymbol{a}^i - \boldsymbol{t}^i_{p,q})^2} \tag{9}$$

If the grid $Z_{p,q}$ is the actual tag position, the theoretical phase difference should be equal to the measured one, which means each $\boldsymbol{a}^i - \boldsymbol{t}^i_{p,q}$ approaches 0. Then the sum of obtained from these difference between the theoretical phase offsets and actual ones should be minimal which leads to the maximized $h_{p,q}$. Conversely, if the tag is not at grid $Z_{p,q}$, the big difference between these two kinds of phase offsets will cause a small value of likelihood. To locate the target tag, every possible grid on H is tested and the grid with highest $h_{p,q}$ is the estimated position of the target tag in advanced model.

3 LAYER DETERMINATION

3.1 Empirical Study

After obtaining the accurate estimated position of each tag through localization model, we could determine the orders of target tags but it is still difficult to determine the tag's layer only by the phase attribute of its signal. To study signal strength indicator (RSSI) value's relevance to the AoA when the positions of target tag and antenna remain unchanged, we conduct a simple experiment in laboratory and the setting is shown in Figure 3(a). We use ϕ to represent the angle between the tag and the antenna's direction in XoY plane, therefore the tag is faced to the antenna when ϕ is 0. Then the relationship between ϕ and RSSI value of target tag is shown in Figure 3(b) as the antenna turns around at the same position. Experimental result shows that RSSI reaches its peak value when ϕ approaches to 0 and it decreases as the absolute value of ϕ become bigger. This study indicates that RSSI values are highly related with the Angle of Arrival of the backscattered signal from tags which will be used in our layer determination module.

3.2 Layer Distinguishing

In our system, we change the traditional deployment for reader's antenna subtly by changing its orientation for a specific degree as

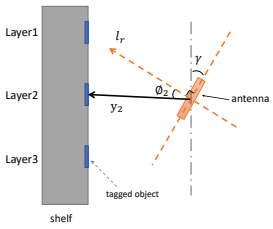

(a) Antenna Deployment

Layer	Radial Distance	RSSI
1	++	++
2	+	+/++
3	++	-

(b) Features For Different Indicators

Figure 4: Layer Distinguishing

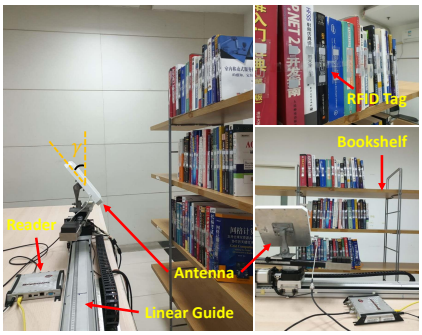

Figure 5: Experimental Setting

illustrated in Figure 4(a). The y_i denotes the radial distance between the tags on i^{th} layer to the antenna. ϕ_i represents the included angle between the line from i^{th} layer' tags to the antenna and the orientation of antenna. γ is the rotation angle of the antenna. Note that tags on different layers have different radial directions in three-dimensional space. It is obvious that $|\phi_3| > |\phi_1|$ leading to the difference between RSSI values of tags on layer1 and layer3 according to the former empirical study even though $y_1 \approx y_3$. The tags on layer2 could be easily distinguished by the radial distance because $y_2 < y_1, y_3$. In conclusion, we list the features of tags on each layer when the antenna is in front of them at Figure 4(b). When the antenna is faced to tags, it is obvious that the tags on layer1 and layer3 have longer radial distances compared to the tags on layer2. Meanwhile, the RSSI of tags on layer3 are minimum due to its large radial distances and AoA while the tags on layer1 and layer2 have bigger RSSI values because of their smaller radial distance or $|\phi|$. Therefore the layers of all tags can be determinate thanks to the little change in deployment of reader's antenna.

3.3 SVM Training

Since we transfer the layer determination problem to a classification one, a machine learning algorithm could be used to solve it. Suppose we create a set of training data $(\boldsymbol{x}_1, y_1), (\boldsymbol{x}_2, y_2), ..., (\boldsymbol{x}_K, y_K)$ where each one corresponds to a tag and y_k is its class label which is the number of layer for the k^{th} tag actually. $\boldsymbol{x}_k \in \Re^2$ is a feature vector of each tag which can be expressed as $\boldsymbol{x}_k = (y_k, r_k)$. y_k is the radial distance and r_k is the RSSI value when antenna is in front of tag k, which can be extracted from the RSSI data of k^{th} tag. Suppose reader capture a series of RSSI values $\boldsymbol{r} = [r_1, r_2, ...r_{n-1}, r_n]$ at n measuring points remained from localization model for k^{th} tag.

$$s = \arg \min_{1 \le i \le n} |x_i - \hat{x}| \tag{10}$$

where s is the index of the nearest measuring point to the estimated position in lateral direction which should have the maximum value of RSSI theoretically if the lateral estimated position is the ground truth. Then r_k is set to $\boldsymbol{r}_s$.

Next, we choose support vector machines (SVM)[3] to train our data because it is a kind of effective supervised learning algorithm whose kernel function can build in expert knowledge and it provides good generalization when the training sample has some bias which often exists in the realistic scenes. In practice, we utilize LIBSVM [2] which provides many extension of SVM and support multi-label classification, and choose radial basis function as kernel function while other parameters are set as default in LIBSVM.

4 EVALUATION

4.1 Implementation

We adopt ImpinJ Speedway R420 reader, one Laird S9025PR RFID antenna and multiple RFID tags without any hardware or firmware modification. Our system which uses LLRP protocol to connect the RFID reader is implemented in C# on a computer with an Intel Core i7-4790 CPU at 3.6 GHz and 16 GByte memory. Our experimental settings are illustrated in Figure 5.

4.2 Macro-Benchmarks

We implement STPP and Tagoram (DAH algorithm) based on the same hardware with only one antenna for comparisons. To make comparisons, 60 books attached with one RFID tag for each are put on the three layers uniformly. The height of each layer is 0.35 m and the horizontal distance from antenna to the bookshelf is 0.42 m. The antenna rotates for $\pi/4$ in the implement of PRMS.

Layer Distinguishing: We design three cases according to the relationships among the radial distances from the antenna to three layers. *Case 1:* $y_1 > y_2 \approx y_3$; *Case 2:* $y_1 \approx y_3 > y_2$; *Case 3:* $y_1 > y_2 > y_3$. For each case, PRMS collected data from 120 samples to train the SVM model before distinguishing the layer for each book. The spacings between adjacent tags vary from 2 ~ 8 cm to simulate the real scene. As shown in Figure. 6, PRMS is insensitive to the differences in distance among the three layers while Tagoram and STPP acquire a poor performance especially if there are two layer having similar distances to the antenna. Specially, the performance of PRMS degrades in *Case 3* because many tags on layer 1 suffer some signal losses which lead to the reduction of positioning accuracy. However, PRMS still outperforms Tagoram and STPP in *Case 3* and achieves significantly higher average accuracy of 88.0%. Moreover, the experimental results in *Case 3* prove that it is not an advisable choice to distinguish the layer depending on the difference among radial distances of multilayer.

Ordering: To perform this evaluation, we don't consider the layer of each tag and calculate the ordering success rate independently for each layer. We place the RFID tags with spacing of 2 ~ 4 cm, 4 ~ 6 cm and 6 ~ 8 cm on three layer and conduct experiments with the different vertical height of antenna for 5 times to obtain

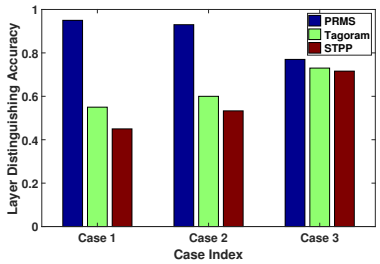

Figure 6: Case Study

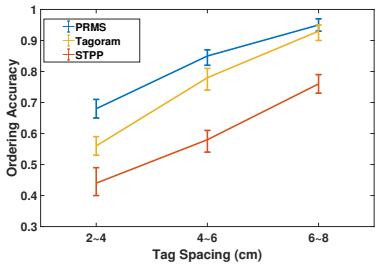

Figure 7: Impact of Tag Spacing

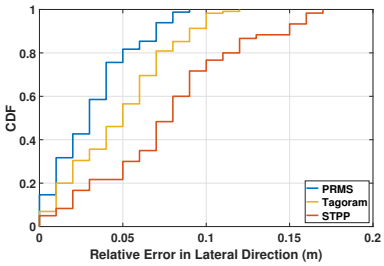

Figure 8: Lateral Relative Error

Table 1: Execution Time of Four Groups. (Unit: ms)

System	Group1	Group2	Group3	Group4
PRMS	5	5	13	13
Tagoram	274	525	640	1252

the mean ordering accuracy. Figure 7 shows that PRMS identifies the right order with a minimum success rate of 68% and a maximum one of 95%. It is obvious that PRMS has better performance in identifying the orders of books compared to STPP and Tagoram.

Relative Localization: Next, we analyse the relative Localization error in lateral direction of these three algorithms to better understand the performance of PRMS. The distances difference between peak positions of two adjacent tags is the estimated distance in STPP. The Cumulative Distributed Function (CDF) of the relative error distances in PRMS, Tagoram and STPP are provided in Figure 8. PRMS achieves a median error distance of 3 cm which is much smaller than those of Tagoram and STPP. Besides, the 90th percentile and the maximum relative positioning error is 7 cm and 9cm respectively.

Execution Time: In this evaluation, we make comparison between two hologram-based algorithms (PRMS and Tagoram with hashtable optimization) in the execution time. We conduct four group and tags are put on different area with size of $1 \times 1\,m^2$, $1 \times 2\,m^2$, $2 \times 1\,m^2$ and $2 \times 2\,m^2$. The length of hologram grid in both PRMS and Tagoram is 0.01 m and the number of sampling points N are 100, 100, 200, 200 respectively for these groups. The execution time of PRMS and Tagoram are provided in Table 1. From the results we can see that the execution time of PRMS is remarkably smaller that that of Tagoram in all groups thanks to a dynamic surveillance plane with a resolution of $P \times Q$ which is a constant (11×101). Tagoram, however, must resize surveillance plane to cover every possible locations of tags and calculate the likelihood of many useless grids for each tag. Another reason is that Tagoram adopts frequent complex exponent operations in implement.

5 CONCLUSIONS

In this paper, we present PRMS, an RFID-based localization system which uses both RSSI and phase information from backscatter signal of RFID tags for localization with a single antenna. Firstly, a basic localization model is proposed to obtain initial estimated locations for RFID tags by measuring the phase differences between each adjacent observation points. Besides, we design an advanced model which employs hologram to improve the performance and reduces the computational complexity by creating a dynamic surveillance plane. The key insight is transfer the part of localization problem to a classification one and utilize a supervised machine learning algorithm to solve it. PRMS can give both the layer of RFID tagged object and its order at this layer simultaneously. Extensive experiments demonstrate that PRMS could achieve 93% layer determination accuracy and 84% ordering accuracy at low (2 ∼ 8cm) spacings.

REFERENCES

[1] Salah Azzouzi, Markus Cremer, Uwe Dettmar, and Rainer Kronberger. 2011. New measurement results for the localization of UHF RFID transponders using an Angle of Arrival (AoA) approach. In *IEEE International Conference on Rfid*. 91–97.

[2] Chih-Chung Chang and Chih-Jen Lin. 2011. LIBSVM: A library for support vector machines. *ACM Transactions on Intelligent Systems and Technology* 2 (2011), 27:1–27:27. Issue 3. Software available at http://www.csie.ntu.edu.tw/~cjlin/libsvm.

[3] Corinna Cortes and Vladimir Vapnik. 1995. Support-vector networks. *Machine Learning* 20, 3 (01 Sep 1995), 273–297. https://doi.org/10.1007/BF00994018

[4] Joshua D. Griffin and Gregory D. Durgin. 2009. Complete Link Budgets for Backscatter-Radio and RFID Systems. *IEEE Antennas & Propagation Magazine* 51, 2 (2009), 11–25.

[5] Gang Li, Daniel Arnitz, Randolf Ebelt, Ulrich Muehlmann, Klaus Witrisal, and Martin Vossiek. 2011. Bandwidth dependence of CW ranging to UHF RFID tags in severe multipath environments. In *IEEE International Conference on Rfid*. 19–25.

[6] Tianci Liu, Lei Yang, Xiang Yang Li, Huaiyi Huang, and Yunhao Liu. 2015. TagBooth: Deep shopping data acquisition powered by RFID tags. In *Computer Communications*. 1670–1678.

[7] Tianci Liu, Lei Yang, Qiongzheng Lin, Yi Guo, and Yunhao Liu. 2014. Anchor-free backscatter positioning for RFID tags with high accuracy. In *IEEE International Conference on Computer Communications, 2014 Proceedings IEEE*. 379–387.

[8] Robert Miesen, Fabian Kirsch, and Martin Vossiek. 2011. Holographic localization of passive UHF RFID transponders. In *IEEE International Conference on Rfid*. 32–37.

[9] A. Parr, R. Miesen, and M. Vossiek. 2013. Inverse SAR approach for localization of moving RFID tags. In *IEEE International Conference on Rfid*. 104–109.

[10] Longfei Shangguan and Kyle Jamieson. 2016. The Design and Implementation of a Mobile RFID Tag Sorting Robot. In *International Conference on Mobile Systems, Applications, and Services*. 31–42.

[11] Longfei Shangguan, Zheng Yang, Alex X Liu, Zimu Zhou, and Yunhao Liu. 2015. Relative localization of RFID tags using spatial-temporal phase profiling. In *Usenix Conference on Networked Systems Design and Implementation*.

[12] Ge Wang, Qian Chen, Longfei Shangguan, Ding Han, Jinsong Han, Nan Yang, Xi Wei, and Jizhong Zhao. 2017. HMRL: Relative Localization of RFID Tags with Static Devices. In *IEEE International Conference on Sensing, Communication, and NETWORKING*. 1–9.

[13] Jue Wang, Fadel Adib, Ross Knepper, Dina Katabi, and Daniela Rus. 2013. RF-compass:robot object manipulation using RFIDs. In *International Conference on Mobile Computing & NETWORKING*. 3–14.

[14] Jue Wang and Dina Katabi. 2013. Dude, where's my card?: RFID positioning that works with multipath and non-line of sight. *Computer Communication Review* 43, 4 (2013), 51–62.

[15] Lei Yang, Yekui Chen, Xiang Yang Li, Chaowei Xiao, Mo Li, and Yunhao Liu. 2014. Tagoram: real-time tracking of mobile RFID tags to high precision using COTS devices. In *International Conference on Mobile Computing and NETWORKING*. 237–248.